

Coupled mode theory for photonic crystal cavity-waveguide interaction

Edo Waks and Jelena Vuckovic

*E.L. Ginzton Laboratories
Stanford University
Stanford, CA 94305
edo@stanford.edu*

Abstract: We derive a coupled mode theory for the interaction of an optical cavity with a waveguide that includes waveguide dispersion. The theory can be applied to photonic crystal cavity waveguide structures. We derive an analytical solution to the add and drop spectra arising from such interactions in the limit of linear dispersion. In this limit, the spectra can accurately predict the cold cavity quality factor (Q) when the interaction is weak. We numerically solve the coupled mode equations for the case of a cavity interacting with the band edge of a periodic waveguide, where linear dispersion is no longer a good approximation. In this regime, the density of states can distort the add and drop spectra. This distortion can lead to more than an order of magnitude overestimation of the cavity Q.

© 2005 Optical Society of America

OCIS codes: (230.7400) Waveguides, slab; (230.5750) Resonators.

References and links

1. M. Loncar et al. "Low-threshold photonic crystal laser." *App. Phys. Lett.* **81**, 2680–2682 (2002).
2. Y. Akahane et al. "Design of a channel drop filter by using a donor-type cavity with high-quality factor in a two-dimensional photonic crystal slab" *App. Phys. Lett.* **82**, 1341–1343 (2003).
3. J. Vuckovic and Y. Yamamoto. "Photonic crystal microcavities for cavity quantum electrodynamics with a single quantum dot," *App. Phys. Lett.* **82**, 2374–2376 (2003).
4. T. Asano et al. "Investigation of channel-add/drop-filtering device using acceptor-type point defects in a two-dimensional photonic-crystal slab," *App. Phys. Lett.* **83**, 407–409 (2003)
5. T. Asano et al. "A channel drop filter using a single defect in a 2d photonic crystal slab - defect engineering with respect to polarization mode and ratio of emissions from upper and lower sides," *J. Lightwave Technol.* **21**, 1370–1376 (2003)
6. C. Seassal et al. "Optical coupling between a two-dimensional photonic crystal-based microcavity and single-line defect waveguide on in-plane membranes," *IEEE J. Quantum Electron.* **38** 811–815 (2002)
7. B.K. Min, J.E. Kim, and H.Y. Park. "Channel drop filters using resonant tunneling processes in two-dimensional triangular lattice photonic crystal slabs," *Opt. Commun.* **237** 59–63 (2004)
8. M.F. Yanik and S. Fan. "High-contrast all-optical bistable switching in photonic crystal microcavities," *App. Phys. Lett.* **83**, 2739 (2003)
9. C. Manolatou et al. "Coupling of modes analysis of resonant channel add-drop filters," *IEEE J. Quantum Electron.* **35**, 1322 (1999)
10. Y. Xu et al. "Scattering-theory analysis of waveguide-resonator coupling," *Phys. Rev. E* **62**, 7389–7404 (2000)
11. S. Olivier et al. "Cascaded photonic crystal guides and cavities: spectral studies and their impact on integrated optics design," *IEEE J. Quantum Electron.* **38**, 816–824 (2002)
12. G.H. Kim et al. "Coupling of small, low-loss hexapole mode with photonic crystal slab waveguide mode," *Opt. Express* **12**, 6624–6631 (2004)
13. M. Okano, S. Kako, and S. Noda. "Coupling between a point-defect cavity and a line-defect waveguide in three-dimensional photonic crystal," *Phys. Rev. B* **68**, 235110 (2003)
14. Ziyang Zhang Min Qiu. "Compact in-plane channel drop filter design using a single cavity with two degenerate modes in 2d photonic crystal slabs," *Opt. Express* **13**, 2596–2604 (2005)

15. Y. Akahane et al. "High-q photonic nanocavity in a two-dimensional photonic crystal," *Nature* **425**, 944–947 (2003)
 16. A. Yariv. *Optical Electronics*. Saunders College Publishing, Philadelphia, 1991.
-

1. Introduction

High-Q photonic crystal (PC) resonators have recently become a subject of great interest. Such cavities have important applications for low threshold lasers, high finesse filters, as well as experiments in cavity quantum electrodynamics (CQED) [1, 2, 3]. One advantage of using PC resonators is that they can be easily integrated with PC based waveguide structures. This is important for a variety of applications, including filtering [4, 5, 6, 7], switching [8], and integrated optical processing.

The interaction of a cavity resonator with a waveguide system has been theoretically studied previously in [11, 12, 13, 14]. These works use finite difference time domain (FDTD) methods to simulate a single specific system. It is difficult to infer from such an analysis the parameters which are important for efficient coupling. Other works consider coupled mode or scattering analysis of cavity-waveguide interaction [9, 10]. But these works consider waveguides with continuous translation symmetry and ignore waveguide dispersion. These approximations are often good for optical fiber waveguides, but do not necessarily apply to PC based waveguides. PC waveguides are periodic in the direction of propagation, and hence exhibit discrete instead of continuous translation symmetry. Because of the discrete translation symmetry, the modes of the waveguide are no longer simple travelling waves. Instead, they take on the form of Bloch states. Another consequence of the waveguide periodicity is that it features an energy stop-band. At the edge of the stop band, the group velocity goes to zero and the dispersion becomes important in characterizing the interaction between the cavity and waveguide. The properties of the interaction near the band edge are particularly important when using photonic crystal cavities formed by single or multiple hole row defects, because these cavities are primarily coupled to waveguide modes near the band edge.

The main goal of this paper is to investigate the interaction of photonic crystal based cavities and waveguides using coupled mode theory as in [9]. However, in order to apply coupled mode analysis, we must properly incorporate dispersion, which plays an important role in photonic crystal waveguides. One of the main results of this paper is a set of coupled mode equations that include dispersion and properly handle the Bloch mode structure of the waveguide modes. Once this is derived, we can apply the theory to realistic photonic crystal based systems.

We first derive the equations of motion for the coupled mode system. After deriving these equations, we solve the system analytically for the special case where the waveguide dispersion relation can be approximated by linear dispersion. Expressions for the add filter and drop filter spectra are explicitly given. When the dispersion relation can no longer be approximated as linear, as in the case of a periodic waveguide near the stop band, an analytical solution becomes too difficult to derive. Instead, we simulate the equations of motion numerically to find the solution.

Our simulations focus on the drop filtering spectrum of the system. Drop filtering is an important operation to analyze because it is often used to measure the cavity quality factor (Q) [15]. To properly interpret such results, it is important to understand the limits under which these measurements can be used to infer Q. We investigate two cases of waveguides that feature stop-bands. The first is a waveguide with weak periodicity in the direction of propagation. In this limit, we have an analytical expression for waveguide dispersion, which can be directly plugged into the coupled mode equations. Although weak periodicity is rarely a good approximation for photonic crystals, it provides a good toy model of a structure with a stop-band, and elucidates much of the physical intuition about the problem. In the second case, we apply the

coupled mode theory to the realistic case of a row-defect photonic-crystal waveguide coupled to a three-hole defect cavity. The modes of the cavity and waveguide, along with the waveguide dispersion relation, are first calculated using FDTD simulation. These simulations are used to calculate the coupling coefficients which enter into the coupled mode theory. The system is then simulated, giving what we believe to be an accurate analysis of a real experiment using such structures. In both cases, we show that when the cavity is resonant near the stop-band, the cavity Q can be overestimated by more than an order of magnitude. This is because the interaction of the cavity with the waveguide is determined by both the cavity spectral function, as well as the waveguide density of states. Near the band edge, the density of states diverges leading to a sharp spectral feature that is unrelated to cavity properties.

2. Coupled mode theory

We begin the derivation of the coupled mode equations with the wave equation

$$\nabla \times \nabla \times \vec{\mathbf{E}} + \frac{\varepsilon(\vec{\mathbf{r}})}{c^2} \frac{\partial^2 \vec{\mathbf{E}}}{\partial t^2} = 0 \quad (1)$$

where $\varepsilon(\mathbf{r})$ is the relative dielectric constant, and c is the speed of light in vacuum. We define ε_c as the relative dielectric constant for the cavity, ε_w as the dielectric constant for the waveguide, and ε_t for the coupled system. We assume the waveguide dielectric constant to be periodic. Thus, the solutions to Eq. (1) with $\varepsilon = \varepsilon_w$, denoted $\vec{\mathbf{E}}_w$, must satisfy the Bloch theorem, and hence take on the form

$$\vec{\mathbf{E}}_w = \vec{\mathbf{B}}_{\mathbf{k}}(\mathbf{r}) e^{i(\omega(k)t - kz)} \quad (2)$$

where $\vec{\mathbf{B}}_{\mathbf{k}}$ are Bloch states that have the same periodicity as ε_w , k is the crystal momentum, and z the direction of propagation in the waveguide. The cavity mode, which is the solution to Eq. (1) with $\varepsilon = \varepsilon_c$ as the index, is defined as $\vec{\mathbf{A}}(\mathbf{r})$.

The dynamics of the coupled system are determined by setting $\varepsilon = \varepsilon_t$ in Eq. (1). Using the standard arguments of coupled mode theory [16], we assume the solution of the coupled system to take on the form

$$\vec{\mathbf{E}} = a(t) \vec{\mathbf{A}}(\mathbf{r}) e^{i\omega_c t} + \int dk \vec{\mathbf{B}}_{\mathbf{k}}(\mathbf{r}) e^{i\omega(k)t} \left[b(k, t) e^{-ikz} + c(k, t) e^{ikz} \right] \quad (3)$$

where $a(t)$ is the slowly varying component of the cavity, and $b(k, t)$ and $c(k, t)$ are slowly varying components of the forward and backward propagating Bloch states respectively. Plugging the above solution back into Eq. (1), we derive the coupled mode equations

$$\frac{da}{dt} = -i \int dk \frac{\omega^2(k)}{\omega_c} e^{i\Delta\omega(k)t} [b(k, t) \kappa_{ba}(k) + c(k, t) \kappa_{ba}(-k)] - \nu a + P_c e^{i(\omega_p - \omega(k))t} \quad (4)$$

$$\frac{db(k)}{dt} = -i \frac{\omega_c^2 \kappa_{ab}(k)}{\omega(k)} a e^{-i\Delta\omega(k)t} + P_w(k) e^{i(\omega_p - \omega(k))t} - \eta b(k) \quad (5)$$

$$\frac{dc(k)}{dt} = -i \frac{\omega_c^2 \kappa_{ab}(-k)}{\omega(k)} a e^{-i\Delta\omega(k)t} + P_w(-k) e^{i(\omega_p - \omega(k))t} - \eta c(k) \quad (6)$$

In the above equations, ν is a phenomenological decay constant which is added to account for the finite lifetime of the cavity resulting from mechanisms other than cavity-waveguide coupling. P_c and $P_w(k)$ are external driving terms that can potentially drive the cavity or waveguide at a frequency ω_p . The damping term η is also included to give the waveguide modes a finite lifetime. In the analytical calculations we take the limit $\eta \rightarrow 0$. In the numerical simulations,

however, we set this damping term to a very small value in order to have a well defined steady state solution. The coupling constants are given by

$$\kappa_{ba}(k) = \frac{\int d\mathbf{r} \frac{\Delta\epsilon_w(\mathbf{r})}{c^2} e^{-ikz} \vec{\mathbf{B}}_{\mathbf{k}} \cdot \vec{\mathbf{A}}^*}{\int d\mathbf{r} \frac{2\epsilon_t(\mathbf{r})}{c^2} |\vec{\mathbf{A}}|^2} \quad (7)$$

$$\kappa_{ab}(k) = \int d\mathbf{r} \frac{\Delta\epsilon_c(\mathbf{r})}{c^2} e^{-ikz} \vec{\mathbf{A}} \cdot \vec{\mathbf{B}}_{\mathbf{k}}^* \quad (8)$$

where $\Delta\epsilon_{c,w} = \epsilon_t - \epsilon_{c,w}$.

3. Linear dispersion

The solution to the above set of coupled equations strongly depends on the waveguide dispersion relation, which relates $\omega(k)$ to k . For some systems, we can assume that this relation is linear, taking on the form

$$\omega(k) = \omega_0 + V_g(k - k_0) \quad (9)$$

where V_g is the group velocity. When this linearized approximation is valid, an analytical solution can be derived for Eq. (4)-(6). This solution is most easily obtained using the method of Laplace transforms. We take the Laplace transform in time of Eq. (5) and Eq. (6) and plug into Eq. (4). We make the additional approximation

$$\frac{1}{(\omega_{c,p} - \omega(k)) + is} \approx P \left[\frac{1}{\omega_{c,p} - \omega(k)} \right] + i\pi\delta(\omega_{c,p} - \omega(k)) \quad (10)$$

where P represents the Cauchy principal value of the expression. This leads to

$$a(s) = \frac{1}{s + \lambda + \Gamma + i\delta\omega} \left(a_0 + \frac{P_c + J}{(s - i(\omega_p - \omega_c))} \right) \quad (11)$$

where, a_0 is the initial cavity field, and the other constants are given by

$$\begin{aligned} \Gamma &= \frac{2\pi Re \{ \kappa_{ab}(k(\omega_c)) \kappa_{ba}(k(\omega_c)) \}}{V_g} \\ \delta\omega &= P \left(\int dk \frac{2\omega(k) Re \{ \kappa_{ab}(k(\omega_c)) \kappa_{ba}(k(\omega_c)) \}}{V_g(\omega(k) - \omega_c)} \right) \\ J &= P \left(\int dk \frac{2\omega(k) \kappa_{ab}(k)}{\omega(k) - \omega_c} \right) - i \frac{\pi\omega_c (\kappa_{ab}(k(\omega_c)) P_w(k(\omega_c)) + \kappa_{ab}(-k(\omega_c)) P_w(-k(\omega_c)))}{V_g} \end{aligned}$$

The above expressions also assume that $A(r)$ is a real function, so that $\gamma(k) = \gamma(-k)$.

Consider first the simple example of a ring-down experiment with no external sources, meaning $P_w = P_c = 0$. The cavity is assumed to contain an initial field $a(0)$ at time 0. The solution of the cavity field is obtained from the equations of motion to be

$$a(t) = a(0)e^{-(v+\Gamma)t} \quad (12)$$

The above solution has a simple interpretation. The constant v is the rate at which the cavity field escapes into leaky modes, while Γ is the rate at which the cavity field escapes into the waveguide. The total decay rate of the cavity field is simply the sum of these two rates. It is important to note that the coupling rate into the waveguide is inversely proportional to the group velocity. This dependence is simply a reflection of the increased interaction time between the cavity and waveguide at slower group velocities.

Next consider an add filter experiment, where both cavity and waveguide are initially empty and $P_w = 0$. One can show that the cavity source term will drive the waveguide field to a steady state value given by

$$|b_k(t)|^2 = \frac{|\pi\kappa_{ab}P_c|^2}{\omega(k)^2} \frac{1}{(\omega_p - \omega_c + \delta\omega)^2 + (\nu + \Gamma)^2} \quad (13)$$

The field features the Lorentzian line-shape expected from an exponential decay process. Similarly, one can derive the drop spectrum of the waveguide by setting $P_c = 0$. In this case the waveguide spectrum is

$$|b_k(t)|^2 = |P_w(k_p)|^2 \left| \left(1 - \frac{J}{i(\omega_p - \omega_c) + \nu + \Gamma} \right) \right|^2 \quad (14)$$

which is an inverse Lorentzian.

4. Weakly periodic waveguides

In the linear dispersion limit there is little qualitative difference between the results presented above and those for the single mode analysis in Ref. [9]. The main distinction is that with linear dispersion, the interaction strength is inversely proportional to the group velocity. But in many cases, one cannot linearly approximate the dispersion relation. One such case is a photonic crystal waveguide, which is periodic in the direction of propagation and therefore features a stop-band. At the edge of the stop-band, the group velocity goes to zero, at which point the dispersive properties of the waveguide become important.

Before treating the full case of photonic crystal structures, we start with a simpler case of a waveguide with weak periodicity in the direction of propagation. The dispersion relation of such a structure can be approximated as [16]

$$\omega_k = \frac{c}{n_{eff}} \left(\frac{\pi}{a} - \sqrt{D^2 + \left(k - \frac{\pi}{a}\right)^2} \right) \quad (15)$$

Above, a is the periodicity of the lattice, D is the size of the bandgap (related to the index contrast of the periodicity), and n_{eff} is an effective index of refraction. This dispersion relation is plotted in Fig. 1 for the case $D = 0.1$.

To get an intuitive understanding of how a cavity will interact with a waveguide featuring such a dispersion, we first note that the cavity only couples well to waveguide modes which conserve both energy and momentum. Because the cavity field is confined in both space and energy, a cavity mode can be represented as a region in the dispersion diagram. In this work, we consider cavities which are spatially localized to only a few wavelengths, but have quality factors of hundreds or more. These cavities are highly localized in energy, and very delocalized in momentum. We thus represent them as an elongated ellipse on the dispersion diagram. In Fig. 1 four different cavity resonant frequencies have been drawn. Cavities with resonant frequencies of 0.35 and 0.4 lie in the nearly linear region of the dispersion diagram. This regime can be treated analytically, as we have done in the previous section. The interaction between the cavity and waveguide mode is primarily determined by energy conservation. If the waveguide is initially excited, modes which are near the cavity resonance will preferentially be scattered. The transmitted spectrum can then be used to infer the cavity spectrum, as Eq. (14) indicates.

Next, consider the cavity with a resonant frequency of 0.45, which is right at the band edge of the waveguide. In this case, the interaction with the waveguide is not simply determined by energy conservation. The cavity scatters more strongly in regions with higher density of states,

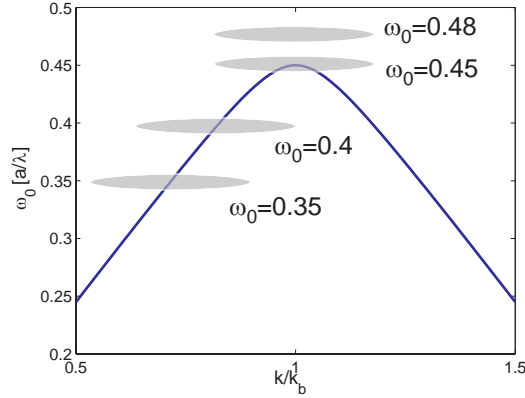


Fig. 1. Dispersion relation for a periodic waveguide.

leading to distortion of the line shape. In this case, the transmission spectrum of the waveguide is no longer a good representation of the cavity spectrum, and may lead to false prediction of the cavity Q . We verify this by numerically simulating Eq. (4)-(6) using the dispersion relation in Eq. (15).

In the simulation, the speed of light is set to $c = 1$, and the effective index of refraction is $n_{eff} = 1$. The bandgap constant is set to $D = 0.1$. We set $\kappa_{ab} = \kappa_{ba} = 10^{-2}$, and assume that these coupling constants are independent of k . This is a good approximation for small cavities which are highly delocalized in momentum. The cavity decay constant is set to 0.01, which corresponds to a cavity Q of 35 for $\omega_0 = 0.35$. This value was selected because it corresponds to a sufficiently narrow linewidth for the simulation, but is not exceedingly narrow that it requires very long simulation times. To simulate drop filtering we set both waveguide and cavity to be initially empty, and pump the waveguide modes with a pump source whose resonant frequency ω_p is swept across the cavity resonance. We set the waveguide modes to have a decay constant $\eta = 0.0005$, which is much smaller than the decay of the cavity, and pump the system until a steady-state value is reached. We then calculate the transmitted power which is defined as

$$P_T = \int_k dk |b(k, t_f)|^2 \quad (16)$$

where t_f is a large enough time for all transients to decay so that the system is in steady state. The transmitted power is normalized by the transmitted power of the waveguide without a cavity. This normalization constant is calculated by evolving the system with $\kappa_{ab} = \kappa_{ba} = 0$.

The transmission as a function of pump frequency is shown in Fig. 2. The transmission is plotted for a cavity resonant frequency of 0.35, 0.4, 0.45, and 0.46. The cavities with resonant frequencies of 0.35 and 0.4 are in the linear dispersion regime, so their drop spectrum is lorentzian as predicted by Eq. (14). The linewidth of the drop spectrum for these two frequencies has a width which corresponds to a decay rate of 0.01, and is therefore completely determined by the cavity lifetime. However, as the cavity resonance approaches the stop-band, as for $\omega_0 = 0.45$, the cavity spectrum significantly narrows. This linewidth distortion is caused by the divergence of the density of states near the band edge. The linewidth when $\omega_0 = 0.45$ corresponds to a quality factor of 180, which is significantly larger than the cold cavity Q of 45. The effect is even more dramatic when $\omega_0 = 0.46$, at which point the cavity resonance is completely inside the bandgap. Despite the fact that the cavity does not resonate with any of the waveguide modes, the extremely high density of states near the band edge still allows the

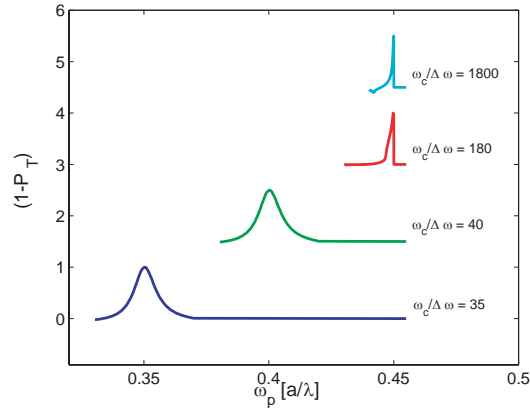


Fig. 2. Inverted waveguide transmission spectrum for different cavity resonant frequencies. Each spectrum has been normalized to its peak value.

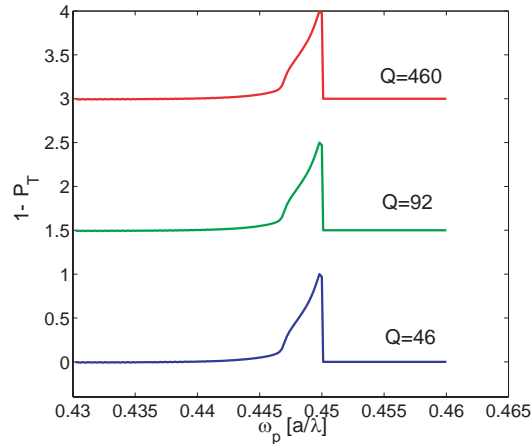


Fig. 3. Drop spectrum for cavity with $\omega_0 = 0.46$ and different quality factors (Q).

cavity to efficiently scatter light. This results in an extremely sharp resonance right at the band edge frequency, whose linewidth corresponds to a Q of 1800.

When the cavity resonance is inside the stop-band of the waveguide, we expect the shape of the transmission spectrum to be largely independent of the cavity Q . This is because only the tail end of the cavity spectrum overlaps with waveguide frequencies, and this tail is predominantly flat. Thus, the cavity spectrum is mainly a reflection of the density of states of the waveguide. To verify this, we set $\omega_0 = 0.46$ and vary the cavity Q . The calculated drop spectra for different Q values are shown in Fig. 3. As can be seen, the linewidth remains almost completely unchanged as we sweep the Q from 46 to 460. We expect this trend to continue as the Q goes up to values of 10,000 and beyond, which are more realistic Q values for photonic crystal micro-cavities.

5. Photonic crystal cavity-waveguide system

We now consider the more realistic case of a photonic crystal cavity-waveguide system. Figure 4 shows an SEM image of the type of system to be analyzed. A waveguide is formed from a row defect in a hexagonal photonic crystal lattice with a periodicity a , slab thickness $d = 0.65a$,

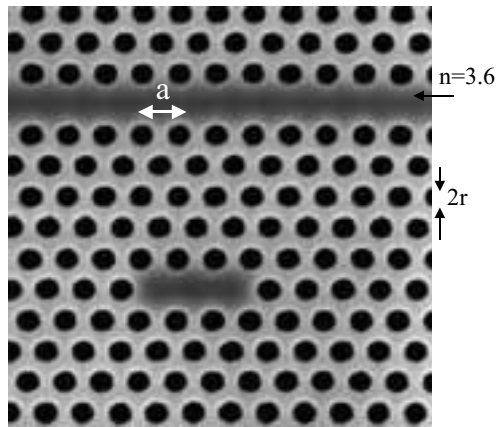


Fig. 4. SEM image of coupled cavity-waveguide system.

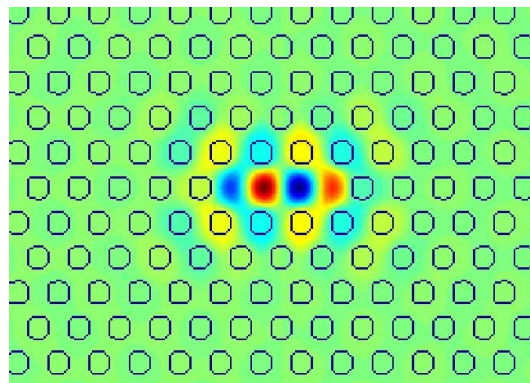


Fig. 5. FDTD simulation of cavity mode. Figure shows z -component of the magnetic field at the center of the slab.

hole radius $r = 0.3a$, and refractive index $n = 3.6$. The waveguide is evanescently coupled to a cavity formed by a three hole defect. Fig. 5 shows three dimensional (3D) FDTD simulations of the cavity mode, which has a normalized resonant frequency of 0.251 in units of a/λ , where λ is the free space wavelength. Figure 6 shows the dispersion relation of the waveguide modes, which are calculated by the same 3D FDTD method. The grey area represents the top of the air band and bottom of the dielectric band for the photonic crystal mirrors. The red line is represents the light-line of the slab waveguide. Any modes above this line will be extremely lossy, as they are not confined by total internal reflection. The white area, which lies approximately between the frequencies 0.23 and 0.33, represents the bandgap region of the mirrors. Waveguiding can only happen in this bandgap region. We see that inside the bandgap there are two waveguide bands, represented by light and dark circles. These two bands cross, meaning that the are of opposite parity and hence do not couple. The insets show the z component of the magnetic field of these two bands at the band edge, taken at the center of the slab. One of the modes has even parity across the center of the waveguide, while the other mode has odd parity. Looking at Fig. 5, one can see that the cavity mode has even parity, and will therefore couple only to the even parity Bloch state. Thus, the odd parity mode can be neglected in the simula-

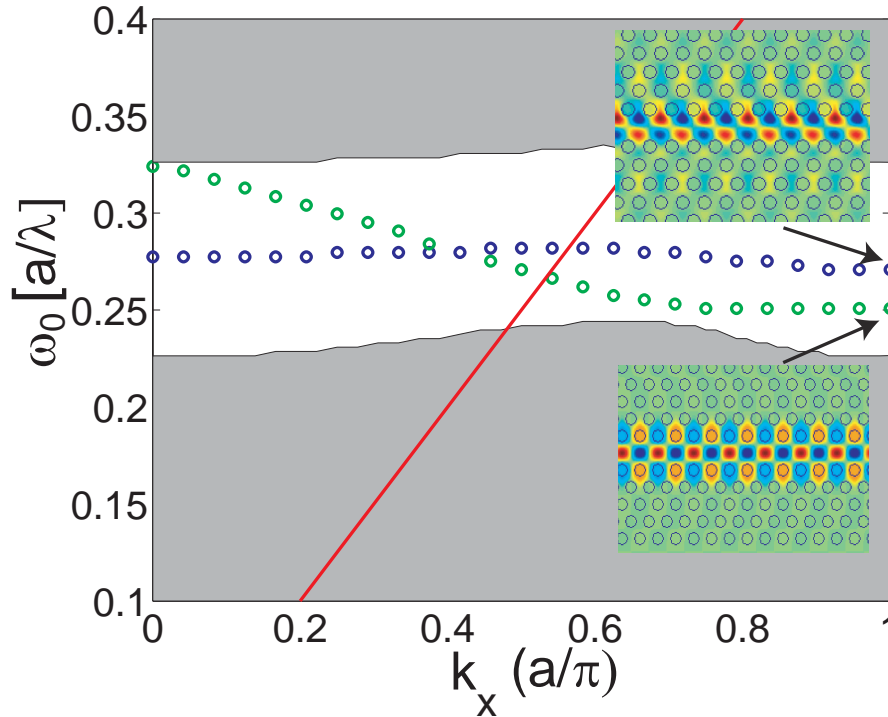


Fig. 6. Dispersion relation for photonic crystal waveguide.

tions. It is important to note that both the even and odd modes feature a nearly flat dispersion near the band edge.

Next, we calculate the coupling coefficients κ_{ab} and κ_{ba} . This is done by first using FDTD simulations to determine the field at the center of the slab waveguide for different in plane momenta. The overlap integrals in Eq. (7) and Eq. (8) are then evaluated numerically for different in plane momenta. The results are shown in Fig. 7. The cavity is most strongly coupled to waveguide modes near $k = \pi/a$, which is the flattest region of the dispersion. The calculated coupling constants are used to simulate the waveguide transmission using the same technique as the weak periodicity waveguide. A three hole defect cavity of the type shown in Fig. 4 has a typical Q of about 2000. Such a high quality factor would require extremely long calculation times to properly simulate. Instead, we set the cavity $Q = 350$. The drop spectrum of the cavity is plotted in Fig. 8. From the full-width half-max bandwidth of the cavity one finds a Q of 1300, which is much larger than the cold cavity Q . The width of the transmission spectrum in Fig. 8 is limited by the spectral resolution of the simulation.

In conclusion, we presented a coupled mode theory for cavity-waveguide interaction which includes waveguide dispersion. In the limit of linearly dispersion, we derived an analytical solution for the cavity decay rate, as well as the add and drop spectra. In this regime, the decay rate into the waveguide is found to be inversely proportional to the group velocity. The add and drop spectra are also found to accurately predict the cavity spectrum in the limit of weak interaction. For the case of nonlinear dispersion, we have numerically solved for the transmission spectrum of the waveguide coupled to the cavity. We investigated waveguides that feature a stop-band, and looked at the behavior near the edge of the stop-band where the group velocity vanishes. The diverging density of states near the band edge can lead to more than

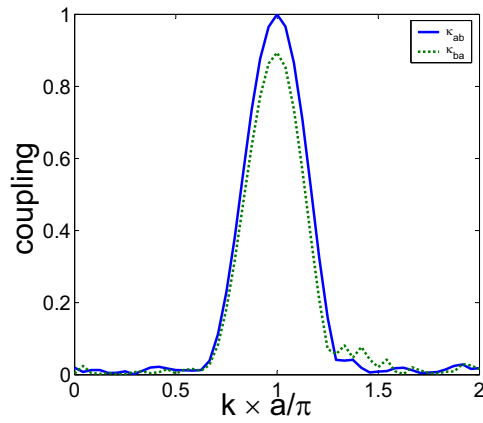


Fig. 7. Calculated coupling strength for cavity-waveguide system.

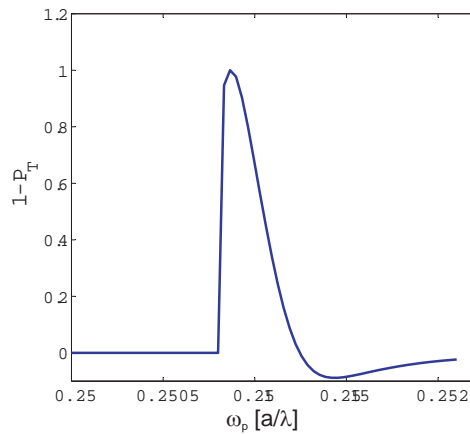


Fig. 8. Transmission spectrum of realistic cavity-waveguide system.

an order of magnitude overestimation of the cavity Q . We believe these results are important in order to better understand general cavity-waveguide interactions in most photonic crystal systems.

This work has been supported by the MURI center for quantum information systems (ARO/ARDA Program DAAD19-03-1-0199) and by a DCI fellowship grant. The authors would also like to thank Dirk Englund for his help with FDTD simulations, and David Fattal for assistance with analytical coupled mode theory solutions.